REPORT DOCUMENTATION PAGE

Form Approved
OMB No. 0704-0188

1. REPORT DATE *(DD-MM-YYYY)*	2. REPORT TYPE	3. DATES COVERED *(From - To)*
	Technical Paper	

4. TITLE AND SUBTITLE

5a. CONTRACT NUMBER
F04611-99-C-0025

5b. GRANT NUMBER

5c. PROGRAM ELEMENT NUMBER

6. AUTHOR(S)

5d. PROJECT NUMBER

5e. TASK NUMBER

5f. WORK UNIT NUMBER

7. PERFORMING ORGANIZATION NAME(S) AND ADDRESS(ES)

ERC

8. PERFORMING ORGANIZATION REPORT

9. SPONSORING / MONITORING AGENCY NAME(S) AND ADDRESS(ES)

Air Force Research Laboratory (AFMC)
AFRL/PRS
5 Pollux Drive
Edwards AFB CA 93524-7048

10. SPONSOR/MONITOR'S ACRONYM(S)

11. SPONSOR/MONITOR'S NUMBER(S)

12. DISTRIBUTION / AVAILABILITY STATEMENT

Approved for public release; distribution unlimited.

13. SUPPLEMENTARY NOTES

14. ABSTRACT

15. SUBJECT TERMS

16. SECURITY CLASSIFICATION OF:			17. LIMITATION OF ABSTRACT	18. NUMBER OF PAGES	19a. NAME OF RESPONSIBLE PERSON
					Leilani Richardson
a. REPORT	b. ABSTRACT	c. THIS PAGE			19b. TELEPHONE NUMBER *(include area code)*
Unclassified	Unclassified	Unclassified	A		(661) 275-5015

2 items enclosed

FILE

MEMORANDUM FOR PRS (In-House/Contractor Publication)

FROM: PROI (STINFO)

05 August 2002

SUBJECT: Authorization for Release of Technical Information, Control Number: **AFRL-PR-ED-TP-2002-198**
Karl Christe (ERC) et al., "Structures of the BrF_4^+ and IF_4^+ Cations"

55194

Inorganic Chemistry
(Deadline: N/A)

(Statement A)

submitter =
- key =

Structures of the BrF_4^+ and IF_4^+ Cations

Ashwani Vij,[†] Fook S. Tham,[§] Vandana Vij,[†] William W. Wilson,[†] and Karl O. Christe *,[†,‡]

Air Force Research Laboratory, Edwards Air Force Base, Edwards, California 93524, University of Southern California Loker Hydrocarbon Research Institute, University Park, Los Angeles, California 90089, and Department of Chemistry, University of California Riverside, California 92521

Abstract

The large discrepancies between the calculated and observed structures for BrF_4^+ and IF_4^+ (J. Am. Chem. Soc. **2001**, *123,* 6338) prompted a redetermination of the crystal structures of $BrF_4^+Sb_2F_{11}^-$ (monoclinic, $P2_1/c$, a = 5.2289(6) Å, b = 14.510(2) Å, c = 14.194(2) Å, • = 90.280(1)°, Z = 4) and $IF_4^+SbF_6^-$ (orthorhombic, *Ibca,* a = 8.2702(9) Å, b = 8.3115(9) Å, c = 20.607(2) Å, Z = 8). It is shown that for BrF_4^+, the large differences were mainly due to large errors in the original experimental data. For $IF_4^+SbF_6^-$, the geometry previously reported for IF_4^+ was reasonably close to that found in this study in spite of a very large R-factor of 0.15 and a refinement in an incorrect space group. The general agreement between the calculated and the redetermined geometries of BrF_4^+ and IF_4^+ is excellent, except for the preferential compression of one bond angle in each ion due to the influence of inter-ionic fluorine bridges. In BrF_4^+, the fluorine bridges are equatorial and compress this angle. In IF_4^+, the nature of the fluorine bridges depends on the counter ion, and either the axial (in $IF_4^+SbF_6^-$) or the equatorial (in $IF_4^+Sb_2F_{11}^-$) bond angle is preferentially compressed. Therefore, the geometries of the free ions are best described by the theoretical calculations.

Introduction

The halogen central atoms in binary halogen fluoride molecules and ions exhibit oxidation states ranging from (+I) to (+VII) and coordination numbers ranging from 1 to 8. These wide ranges render them ideal candidates for exploring molecular structure and bonding. [1-3] In a recent paper, the crystal structure of $ClF_4^+SbF_6^-$ has been reported, and the general trends within the isoelectronic series ClF_4^+, BrF_4^+, IF_4^+, and SF_4, SeF_4, TeF_4, have been evaluated.[4] Whereas the theoretical calculations agreed well with the experimental structures of the neutral molecules and resulted in smooth trends, the crystal structures previously reported for ClF_4^+,[4] BrF_4^+, [5] and IF_4^+ [6,7] strongly deviated from the theoretical predictions and resulted in erratic trends[4] (see Figure 1). Since the crystal structures for BrF_4^+ and IF_4^+ were of low accuracy, it was important to redetermine these structures and to resolve the apparent discrepancies between theory and experiment.

Experimental

Materials and Apparatus. The sample of $BrF_4^+Sb_2F_{11}^-$ was prepared as previously described.[8] Single crystals were obtained by slow sublimation at room temperature over a time period of 30 years. Single crystals of $IF_4^+SbF_6^-$ were obtained in the following manner. In a glove box, a two-fold excess of SbF_5 (19.27 mmol) was loaded into a prepassivated Teflon ampule, fitted with a Hoke stainless steel valve. The ampule was connected to a stainless steel vacuum line[9] and evacuated at –196 °C. Anhydrous HF (3 mL) was condensed onto the SbF_5, followed by freshly distilled IF_5 (9.50 mmol). The reaction mixture was allowed to warm to room temperature for 1 hr. All volatile material was pumped off at room temperature for 12 hr, leaving behind a

white crystalline solid identified as $IF_4^+SbF_6^-$ by material balance (9.50 mmol) and its infrared and Raman spectra.[8]

Crystal Structures of $BrF_4^+Sb_2F_{11}^-$ and $IF_4^+SbF_6^-$. Diffraction quality, colorless crystals of $BrF_4^+Sb_2F_{11}^-$ (**1**) or $IF_4^+SbF_6^-$ (**2**) were immersed into a perfluoro-polyether (PFPE) filled cavity of a culture dish. A crystal was then sucked by capillary force into a 0.3 mm Lindeman capillary tube along with some PFPE oil. The capillary was sealed at both ends and mounted on a goniometer head using a copper pin. The structures of the salts were determined with a Bruker CCD SMART 1000 diffractometer that was controlled by the SMART software.[10] Unit cell parameters were determined at 243 K ($BrF_4^+Sb_2F_{11}^-$) or 233 K ($IF_4^+SbF_6^-$) from three runs of frame data with a scan speed of 30-sec/frame and 30 frames per data run. A complete hemisphere of data was collected at the temperatures described above using 1271 frames at 30 sec/frame, including 50 frames that were collected at the beginning and end of each data collection to monitor crystal decay. Data were integrated using the SAINT[11] software, and the raw data was corrected for absorption using the SADABS[12] program. The structures were solved with the SHELXS-97 program[13] employing the Patterson method and refined anisotropically with the SHELXL-97[14] software incorporated into the SHELXTL 5.1 program[15] (Table 1).

For $BrF_4^+Sb_2F_{11}^-$, the intensity statistics, i.e., the E^2-1 values, indicated a centro-symmetric space group. Furthermore, the absence of 0 k 0 (k = odd) and $h0l$ reflections (l = odd) showed the presence of a 2_1 screw axis and a c-glide plane parallel and perpendicular to the b-axis, respectively. The space group was thus unambiguously assigned as $P2_1/c$.

The determination of the space group for $IF_4^+SbF_6^-$ was not trivial. Initial frame data indicated a body-centered orthorhombic cell (space group *Ibca*) with the following

axes, a = 8.270 Å, b = 8.3115 Å, c = 20.607 Å. Since the a and b values are quite similar, the possibility of a tetragonal unit cell was also examined but rejected based upon the R_{sym} value being twice as large. Furthermore, solution of the structure using the tetragonal option results in a disordered structure flawed by poor geometry, thermal parameters and associated errors, a higher R-value of 0.0675, a poor data to parameter ratio of 8.514, and a high residual electron density. On the other hand, choice of the body-centered orthorhombic cell results in an ordered structure that could be solved in the space group *Ibca* with a lower R-value (0.0241), higher data to parameter ratio, and good thermal and geometrical parameters. Based on these considerations and the observed systematic absences, *Icba* is the correct space group. Although the possibility of a C-centered super lattice cannot be ruled out, it was not further pursued because of satisfactory refinement in *Icba*.

The previously reported[6] tetragonal cell (space group *P4/mmm*) with a = 5.863 Å, c = 10.303 Å can be obtained by transformation of our orthorhombic cell by using a –0.5, –0.5, 0.0, 0.5, –0.5, 0.0, 0.0, 0.0, 0.5 matrix. This, however, skews the • angle to 89.71° and can account for some of the problems encountered with the previous study.

Results and Discussion

Calculated Structures of the free BrF_4^+ and IF_4^+ Cations. Ideally, the XF_4^+ cations possess pseudo-trigonal bipyramidal geometries of C_{2v} symmetry with the third equatorial position being occupied by a sterically active, free valence electron pair.

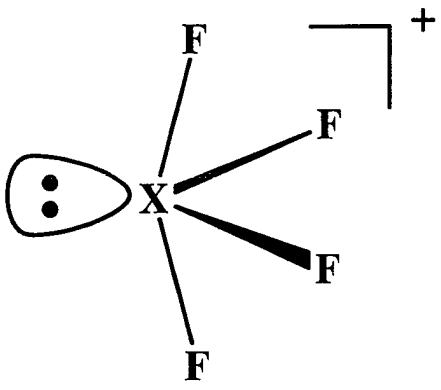

Since the free electron pair domain is more repulsive than those of the fluorine ligands, the angles of both the axial and the equatorial fluorine bond pairs are smaller than the ideal 180° and 120°, respectively. In Table 2, the previously observed[5,7] geometries are compared to the unscaled values calculated[4] for free BrF_4^+ and IF_4^+ at different levels of theory. As can be seen from Table 2 and Figure 1, the agreement between the previously reported experimental and the calculated values is very poor, even if empirical corrections of about 0.01 – 0.04 Å for the overestimates that are typical for each method[4] are applied to the bond lengths.

Crystal Structure of $BrF_4^+Sb_2F_{11}^-$. This compound crystallizes in the monoclinic space group $P2_1/c$. The earlier structural refinement[5] for this compound had used a non-standard setting, $P2_1/a$, and the fluorine atoms had been refined isotropically, resulting in a high R factor of 0.14 and very large uncertainties of up to 0.13 Å in the bond lengths. Therefore, the structure of $BrF_4^+Sb_2F_{11}^-$ was redetermined (Figure 2), and the atomic coordinates and isotropic displacement parameters are listed in Table 3. The most important bond distances and angles are summarized in Table 4. The BrF_4^+ cation adopts the expected distorted trigonal bipyramidal geometry in accordance with the structure (see above) predicted for AX_4E-type species by the VSEPR theory.[16] The F14, F15 atoms

and the lone pair on Br1 form the equatorial plane. As in the case of ClF_4^+,[4] SF_4,[17] and SeF_4,[18] the axial bonds of ~1.73 Å are significantly longer than the equatorial bonds of ~1.66 Å, and their lengths are in excellent agreement with the theoretical predictions given in Table 2. Furthermore, the axial and equatorial F-Br-F angles of 168.9(2)° and 97.5(2)°, respectively, are significantly compressed from the ideal values of 180° and 120°. The coordination around bromine is completed by two close fluorine contacts of 2.414(3) (Br1···F2) and 2.347(3) (Br1···F11A) Å from two $Sb_2F_{11}^-$ anions, resulting in infinite zig-zag chains of alternating cations and anions along the *c*-axis (see Fig. 2). The bridge angle, Br···F-Sb, is ~170° and, if the two fluorine bridges are included in the coordination sphere of bromine, its coordination number becomes 7. This fluorine-bridging mode closely resembles that previously found[4] for $ClF_4^+SbF_6^-$ and results in a preferential compression of the equatorial F-Br-F bond angle.

The geometry of the $Sb_2F_{11}^-$ anion depends strongly on the counter ion and can vary from a linear, eclipsed, D_{4h} symmetry structure to strongly bent, staggered structures with an Sb-F-Sb angle of about 150° and dihedral angles of the equatorial SbF_4 groups of up to 50°.[19] In $BrF_4^+Sb_2F_{11}^-$, the $Sb_2F_{11}^-$ anion is present in a quasi-eclipsed conformation with an almost linear Sb1-F6-Sb2 bond of 175.1(1)°. The Sb1-F6-Sb2 bridge exhibits a slight asymmetry with Sb1-F6 and Sb2-F6 values of 1.998(2) and 2.039(2) Å, respectively. The fluorine atoms that are not involved in bridging have an average Sb-F bond distance of 1.842(3) Å, while the two bonds involving the two Sb-F···Br bridges are elongated to 1.899(3) Å.

Crystal Structure of $IF_4^+SbF_6^-$. Although Baird briefly reported a structure for this compound in 1969,[6] it was solved in the incorrect space group with a very low R factor of 0.15, and no structural detail or complete refinement was ever published. The

structure of $IF_4^+Sb_2F_{11}^-$ has also been reported,[7] but the accuracy was also low (R factor of 0.09) and the bond angles found for IF_4^+ were very different from those reported by Baird. Furthermore, the $IF_4^+Sb_2F_{11}^-$ crystal had been obtained accidentally[7] in a reaction of CrO_2F_2 and SbF_5 with IF_5, and an improved bulk synthesis of this compound was desirable. Our attempt to prepare $IF_4^+Sb_2F_{11}^-$ by a 1:2 reaction of IF_5 and SbF_5 in HF solution resulted in the quantitative formation of $IF_4^+SbF_6^-$ and its crystal structure was determined. It crystallizes in the orthorhombic space group *Ibca*. The crystallographic data, atomic coordinates, equivalent isotropic displacement parameters, most important bond lengths and angles, and structure are given in Tables 1, 5, and 6, and Figure 3, respectively.

The structure of $IF_4^+SbF_6^-$ is predominantly ionic, containing fluorine-bridged IF_4^+ cations and SbF_6^- anions. However, the fluorine bridging in $IF_4^+SbF_6^-$ strongly differs from those in $ClF_4^+SbF_6^-$ and $BrF_4^+Sb_2F_{11}^-$. As can be seen from Figure 3, the IF_4^+ cation forms 4 shorter (2.70 Å) and one longer (3.01 Å) fluorine-bridge with 5 different SbF_6^- anions. This results in a monocapped, distorted square-antiprismatic, nine-coordinate environment around iodine. The imperfection of the square antiprism results from the 4 fluorine ligands of iodine not lying in a plane due to the difference in the F_{ax}-I-F_{ax} and F_{eq}-I-F_{eq} bond angles which also causes the twist angle of the two square faces to be 35.6° and not the ideal 45°. Since the axial fluorine ligands experience a much stronger repulsion from the fluorine bridges than the equatorial ones, the axial F-I-F angle is preferentially compressed, contrary to the preferential compression of the equatorial angles in the $ClF_4^+SbF_6^-$ and $BrF_4^+Sb_2F_{11}^-$ structures.

Packing diagrams of $IF_4^+SbF_6^-$ are shown in Figures 4 and 5. The packing consists of double layers of IF_4^+ cations and SbF_6^- anions, with each IF_4^+ cation bridging four

SbF_6^- anions (see Figure 3) through the four shorter fluorine bridges within the *xy*-plane, resulting in the formation of a network of two-dimensional sheets. These polymeric sheets are interconnected along the *z*-axis by the long I1···F3A fluorine-bridges.

The R(I-F_{ax}) and R(I-F_{eq}) values of 1.849(2) and 1.798(2) Å, respectively, and the equatorial F-I-F bond angle of 103.06(12)° are in excellent agreement with the calculated gas phase values of 1.861 and 1.818 Å, and 103.8°, respectively. The significant deviation of the observed axial F-I-F angle of 149.24(13)° from the calculated values of about 160° is due to the above-mentioned preferential compression of the axial angle by the fluorine bridges.

Whereas the I-F bond lengths in $IF_4^+SbF_6^-$, 1.849(2) and 1.798(2) Å, are in fair agreement with those of 1.85(4) and 1.77(3) Å, previously reported for $IF_4^+Sb_2F_{11}^-$,[7] the corresponding bond angles differ markedly. While in $IF_4^+SbF_6^-$ the equatorial F-I-F angle (103.06(12)°) is close to the calculated one (103.8°), in $IF_4^+Sb_2F_{11}^-$ the axial angle (160.3(1.2)°) is close to the theoretically predicted value of 160°, but the equatorial one (92.4(1.2)°) is much smaller than the predicted one of 103.8°. This discrepancy is due to the different nature of the fluorine bridging in $IF_4^+SbF_6^-$ and $IF_4^+Sb_2F_{11}^-$ (see Figure 6). In the former, the four shorter fluorine bridges are identical, whereas in the latter, there are two pairs of fluorine bridges, F11A/F8A and F7A/F13A, which form very different cone angles of 64 and 118°. The one with the wider cone angle, F7A-I1-F13A, closely approaches and almost eclipses the equatorial fluorine atoms, F3A and F2B, of IF_4^+, thereby preferentially compressing the equatorial F3A-I1-F2B angle.

Conclusion. The present study resolves all the problems raised by the previous study.[4] The revised bond lengths and angles of the ClF_4^+, BrF_4^+, IF_4^+ series (Table 7 and Figure 7) now show excellent agreement with the theoretical predictions, if the

preferential compression of one specific bond angle (equatorial F-X-F in $ClF_4^+SbF_6^-$, $BrF_4^+Sb_2F_{11}^-$, and $IF_4^+Sb_2F_{11}^-$, and axial F-X-F in $IF_4^+SbF_6^-$) in each structure due to strong anion-cation interactions is taken into consideration. Since the nature of the fluorine bridging strongly depends on the counter ion and crystal packing, a different angle may be compressed even for the same cation in different salts. This is demonstrated for $IF_4^+SbF_6^-$ and $IF_4^+Sb_2F_{11}^-$. Taking the relatively unaffected angles of each structure, i.e., the axial F-I-F angle of 160° from $IF_4^+Sb_2F_{11}^-$ and the equatorial F-I-F angle of 103° from $IF_4^+SbF_6^-$, the theoretical predictions for free IF_4^+ are well duplicated. As expected, the angle compression due to fluorine bridging becomes more pronounced with increasing size and softness of the central atom, i.e., it increases from chlorine to iodine. The results of this study demonstrate the value of theoretical calculations for the detection, correction, and rationalization of experimental inconsistencies.

Acknowledgement. The authors thank Dr. Robert Corley for his steady encouragement and the National Science Foundation, the Defense Advanced Projects Agency, and the Air Force Office of Scientific Research for financial support.

Supporting Information Available: Tables of structure determination summary, atomic coordinates, bond lengths and angles and anisotropic displacement parameters of $BrF_4^+Sb_2F_{11}^-$ and $IF_4^+SbF_6^-$ in CIF format. This material is available free of charge via the internet at http://pubs.acs.org.

References

*Author to whom correspondence should be addressed. E-mail address: karl.christe@edwards.af.mil.
† Air Force Research Laboratory.
§ University of California, Riverside.
‡ University of Southern California.

(1) Christe, K. O.; Curtis, E. C.; Dixon, D.A.; *J. Am. Chem. Soc.* **1993,** *115,* 1520.

(2) Christe, K. O.; *Proceedings from the XXIVth Int. Congr. Pure Appl. Chem.* [Proc.] **1974,** *4,* 115.

(3) Christe, K. O.; Wilson, W. W.; Drake, G. W.; Dixon, D.A.; Boatz, J. A.; Gnann, R. *J. Am. Chem. Soc.* **1998,** *120,* 1520.

(4) Christe, K. O.; Zhang, X.; Sheehy, J. A.; Bau, R. *J. Am. Chem. Soc.* **2001,** *123,* 6338.

(5) Lind, M. D.; Christe, K. O. *Inorg. Chem.* **1972**, *11,* 608.

(6) Baird, H. W.; Giles, H. F.; *Acta Cryst.* **1969**, *A25*, S115.

(7) Edwards, A. J.; Taylor, P.; *J. Chem. Soc. Dalton* **1975**, 2174.

(8) Christe, K. O.; Sawodny, W. *Inorg. Chem.* **1973**, *12,* 2879.

(9) Christe, K. O.; Wilson, W. W.; Schack, C. J.; Wilson, R. D. *Inorg. Synth.* **1986**, *24,* 39.

(10) SMART Software for the CCD Detector System, Bruker AXS, Madison, WI, 1999.

(11) SAINT Software for the CCD Detector System, Bruker AXS, Madison, WI, 1999.

(12) SADABS, Program for absorption correction for area detectors, Version 2.01, Bruker AXS, Madison, WI (2000).

(13) Sheldrick, G. M. SHELXS-97, Program for the Solution of Crystal Structure, University of Göttingen, Germany, 1997.

(14) Sheldrick, G. M. SHELXL-97, Program for the Refinement of Crystal Structure, University of Göttingen, Germany, 1997

(15) SHELXTL 5.10 for Windows NT, Program Library for Structure Solution and Molecular Graphics, Bruker AXS, Madison, WI, (1997).

(16) Gillespie, R. J.; Hargittai, I. *The VSEPR Model of Molecular Geometry;* Allyn and Bacon: Boston, 1991.

(17) Tolles, W. M.; Gwinn, W. D. *J. Chem. Phys.* **1962,** *36,* 1119.

(18) Bowater, I. C.; Brown, R. D.;Burden, F. R. *J. Mol. Spectrosc.* **1968,** *28,* 454.

(19) See for example: Willner, H.; Bodenbinder, M.; Broechler, R.; Hwang, G.; Rettig, S. J.; Trotter, J.; von Ahsen, B.; Westphal, U.; Jonas, V.; Thiel, W.; Aubke, F. *J. Am. Chem. Soc.* **2001,** *123,* 588; and references cited therein.

Table 1. Crystal Data for $BrF_4^+Sb_2F_{11}^-$ and $IF_4^+SbF_6^-$

	$BrF_4^+Sb_2F_{11}^-$	**$IF_4^+SbF_6^-$**
chemical formula	BrF15Sb2	F10ISb
fw	608.41	438.65
T, K	243(2)	233(2)
space group	$P2_1/c$	*Ibca*
a, Å	5.2289(6)	8.2702(9)
b, Å	14.510(2)	8.3115(9)
c, Å	14.194(2)	20.607(2)
• , *deg*	90.280(2)	90
V, Å^3	1076.9 (2)	1416.5(3)
Z	4	8
• , mm^{-1}	8.920	8.396
• $_{calc,}$ g cm^{-3}	3.753	4.114
R1,[a] *wR2*[b] [*I*>2• (*I*)]	0.0275, 0.0702	0.0241, 0.0654
R1,[a] *wR2*[b] (all data)	0.0344, 0.0735	0.0266, 0.0679

[a] $R1 = (\bullet\ (F_0-F_c)/F_0)$. [b] $wR2 = [\bullet\ (w(F_0-F_c)^2)w/F_0^2)]^{1/2}$.

Table 2. Previously Observed and Calculated Geometries[a] for BrF_4^+ and IF_4^+

	BrF_4^+				IF_4^+			
	obsd[b]	calcd[d]			obsd[c]	calcd[d]		
	$BrF_4^+Sb_2F_{11}^-$	B3LYP	MP2	CCSD(T)	$IF_4^+Sb_2F_{11}^-$	B3LYP	MP2	CCSD(T)
r ($X-F_{eq}$)	1.77(12)	1.700	1.672	1.683	1.77(3)	1.838	1.818	1.823
r ($X-F_{ax}$)	1.86(12)	1.749	1.728	1.732	1.85(4)	1.875	1.861	1.863
< ($F_{eq}-X-F_{eq}$)	95.5(50)	104.9	104.9	105.4	92.4(12)	106.8	103.8	104.2
< ($F_{ax}-X-F_{ax}$)	173.5(61)	168.8	168.2	167.2	160.3(12)	158.3	161.2	160.3

[a] Bond distances in Å, angles in degrees. [b] Data from ref 5. [c] Averaged bond lengths from ref 7. [d] Data from ref 4; the following basis sets were used for all calculations: Br: DFT-DZVP + f(0.552); I: DFT-DZVP + f(0.486); F: -311 + G(2d).

Table 3. Atomic Coordinates (x 10^4) and Equivalent Isotropic Displacement Parameters ($Å^2$x 10^3) for $BrF_4^+Sb_2F_{11}^-$. U(eq) is Defined as one Third of the Trace of the Orthogonalized U^{ij} Tensor.

	x	y	z	U(eq)
Sb(1)	5297(1)	6472(1)	3518(1)	23(1)
Sb(2)	2557(1)	8534(1)	5130(1)	22(1)
Br(1)	9167(1)	8510(1)	1861(1)	26(1)
F(1)	6574(7)	5587(2)	2720(2)	57(1)
F(2)	6881(5)	7453(2)	2865(2)	36(1)
F(3)	8081(6)	6430(2)	4312(2)	43(1)
F(4)	3511(6)	5655(2)	4262(2)	50(1)
F(5)	2400(5)	6688(2)	2798(2)	43(1)
F(6)	3984(5)	7462(2)	4366(2)	43(1)
F(7)	1149(6)	9424(2)	5882(2)	48(1)
F(8)	5461(6)	8373(2)	5849(2)	43(1)
F(9)	4238(6)	9286(2)	4287(2)	43(1)
F(10)	-224(6)	8436(2)	4329(2)	38(1)
F(11)	1073(5)	7564(2)	5847(2)	37(1)
F(12)	12022(7)	8638(2)	2465(2)	52(1)
F(13)	6324(6)	8613(2)	1243(2)	52(1)
F(14)	7971(6)	9297(2)	2590(2)	43(1)
F(15)	10410(5)	9237(2)	1077(2)	40(1)

Table 4. Bond Lengths and Angles for $BrF_4^+Sb_2F_{11}^-$.

Bond Lengths (Å)

Sb(1)-F(3)	1.837(3)	Sb(2)-F(9)	1.845(3)
Sb(1)-F(1)	1.840(3)	Sb(2)-F(10)	1.847(3)
Sb(1)-F(4)	1.844(3)	Sb(2)-F(11)	1.905(3)
Sb(1)-F(5)	1.850(3)	Sb(2)-F(6)	2.039(2)
Sb(1)-F(2)	1.892(3)	Br(1)-F(14)	1.664(3)
Sb(1)-F(6)	1.998(2)	Br(1)-F(15)	1.667(3)
Sb(2)-F(7)	1.832(3)	Br(1)-F(12)	1.728(3)
Sb(2)-F(8)	1.840(3)	Br(1)-F(13)	1.729(3)

Bond Angles (°)

F(3)-Sb(1)-F(1)	93.75(15)	F(8)-Sb(2)-F(10)	167.58(15)
F(3)-Sb(1)-F(4)	91.68(14)	F(9)-Sb(2)-F(10)	91.31(13)
F(1)-Sb(1)-F(4)	95.18(16)	F(7)-Sb(2)-F(11)	92.49(14)
F(3)-Sb(1)-F(5)	171.32(14)	F(8)-Sb(2)-F(11)	86.98(13)
F(1)-Sb(1)-F(5)	94.39(15)	F(9)-Sb(2)-F(11)	168.57(13)
F(4)-Sb(1)-F(5)	90.57(13)	F(10)-Sb(2)-F(11)	87.17(12)
F(3)-Sb(1)-F(2)	88.75(12)	F(7)-Sb(2)-F(6)	175.13(13)
F(1)-Sb(1)-F(2)	93.53(15)	F(8)-Sb(2)-F(6)	83.96(12)
F(4)-Sb(1)-F(2)	171.23(14)	F(9)-Sb(2)-F(6)	85.94(13)
F(5)-Sb(1)-F(2)	87.76(12)	F(10)-Sb(2)-F(6)	84.43(12)
F(3)-Sb(1)-F(6)	85.89(12)	F(11)-Sb(2)-F(6)	82.64(11)
F(1)-Sb(1)-F(6)	178.17(15)	F(14)-Br(1)-F(15)	97.48(16)
F(4)-Sb(1)-F(6)	86.63(13)	F(14)-Br(1)-F(12)	86.80(16)
F(5)-Sb(1)-F(6)	85.88(12)	F(15)-Br(1)-F(12)	85.68(15)
F(2)-Sb(1)-F(6)	84.67(11)	F(14)-Br(1)-F(13)	86.09(15)
F(7)-Sb(2)-F(8)	95.69(15)	F(15)-Br(1)-F(13)	86.78(15)
F(7)-Sb(2)-F(9)	98.94(15)	F(12)-Br(1)-F(13)	168.88(16)
F(8)-Sb(2)-F(9)	92.27(13)	Sb(1)-F(6)-Sb(2)	175.11(15)
F(7)-Sb(2)-F(10)	95.50(14)		

Table 5. Atomic Coordinates (x 10^4) and Equivalent Isotropic Displacement Parameters ($Å^2$x 10^3) for $IF_4^+SbF_6^-$. U(eq) is Defined as one Third of the Trace of the Orthogonalized U^{ij} Tensor.

	x	y	z	U(eq)
I(1)	5000	2500	1505(1)	16(1)
Sb(2)	0	2500	857(1)	13(1)
F(1)	3786(2)	1313(2)	2048(1)	27(1)
F(2)	3490(2)	4031(2)	1743(1)	32(1)
F(3)	0	2500	-42(2)	29(1)
F(4)	0	2500	1752(2)	25(1)
F(5)	2238(2)	2069(2)	857(1)	28(1)
F(6)	439(2)	4725(2)	853(1)	28(1)

Table 6. Bond Lengths and Angles for $IF_4^+SbF_6^-$.

Bond Lengths (Å)

I(1)-F(1)#1	1.7981(17)	Sb(2)-F(3)	1.853(4)
I(1)-F(1)	1.7981(17)	Sb(2)-F(6)#2	1.8846(17)
I(1)-F(2)	1.8490(17)	Sb(2)-F(6)	1.8846(17)
I(1)-F(2)#1	1.8490(17)	Sb(2)-F(5)#2	1.8854(17)
Sb(2)-F(4)	1.845(3)	Sb(2)-F(5)	1.8854(17)

Bond Angles (°)

F(1)#1-I(1)-F(1)	103.06(12)	F(6)#2-Sb(2)-F(6)	179.53(12)
F(1)#1-I(1)-F(2)	80.48(9)	F(4)-Sb(2)-F(5)#2	90.00(6)
F(1)-I(1)-F(2)	80.53(8)	F(3)-Sb(2)-F(5)#2	90.00(6)
F(1)#1-I(1)-F(2)#1	80.53(8)	F(6)#2-Sb(2)-F(5)#2	89.82(7)
F(1)-I(1)-F(2)#1	80.48(9)	F(6)-Sb(2)-F(5)#2	90.18(7)
F(2)-I(1)-F(2)#1	149.24(13)	F(4)-Sb(2)-F(5)	90.00(6)
F(4)-Sb(2)-F(3)	180.0	F(3)-Sb(2)-F(5)	90.00(6)
F(4)-Sb(2)-F(6)#2	90.24(6)	F(6)#2-Sb(2)-F(5)	90.18(7)
F(3)-Sb(2)-F(6)#2	89.76(6)	F(6)-Sb(2)-F(5)	89.82(7)
F(4)-Sb(2)-F(6)	90.24(6)	F(5)#2-Sb(2)-F(5)	179.99(12)
F(3)-Sb(2)-F(6)	89.76(6)		

Symmetry transformations used to generate equivalent atoms:

#1 -x+1,-y+1/2,z+0 #2 -x+0,-y+1/2,z+0

Table 7. Comparison of the Experimental with the Calculated MP2 Geometries for the XF_4^+ Cations (X = Cl, Br and I)

	R(X-F_{ax})	R(X-F_{eq})	F_{ax}-X-F_{ax}	F_{eq}-X-F_{eq}
$ClF_4^+SbF_6^-$	1.618(2)	1.530(2)	173.9(1)	103.1(1)
ClF_4^+ (gas)*	1.612	1.543	172.3	107.1
$BrF_4^+Sb_2F_{11}^-$	1.728(3), 1.729(3)	1.664(3), 1.667(2)	168.9(2)	97.5(2)
BrF_4^+ (gas)*	1.728	1.672	168.2	104.9
$IF_4^+SbF_6^-$	1.849(2)	1.798(2)	149.2(1)	103.1(1)
$IF_4^+Sb_2F_{11}^-$ [a]	1.87(4), 1.82(3)	1.76(3), 1.778(3)	160.3(1.2)	92.4(1.2)
IF_4^+ (gas)*	1.861	1.818	161.2	103.8

*Calculated values. [a] Data from ref 7.

Figure Captions

Figure1. A comparison of calculated (green) and previously reported experimental (red and blue) geometries (distances in Å x 10^2, angles in degrees) for ClF_4^+, BrF_4^+, and IF_4^+. For IF_4^+, the red values are those reported for $IF_4^+Sb_2F_{11}^-$,[7] while the blue ones are those for $IF_4^+SbF_6^-$.[6]

Figure 2. Crystal structure of $BrF_4^+Sb_2F_{11}^-$ with the displacement ellipsoids at the 50% probability level. The Br···F bridges result in a preferential compression of the equatorial F-Br-F angle and the formation of infinite zig-zag chains along the *c*-axis.

Figure 3. Crystal structure of $IF_4^+SbF_6^-$ with the displacement ellipsoids at the 50% probability level. The four shorter I···F bridges result in a preferential compression of the axial F-I-F angle and the formation of infinite polymeric sheets in the xy-plane.

Figure 4. Packing diagram for $IF_4^+SbF_6^-$ showing the arrangement of the polymeric sheets that are perpendicular to the yz-paper-plane and their inter-connection through the longer fluorine bridges. The iodine atoms are shown in purple and the antimony atoms in blue.

Figure 5. Crystal lattice of $IF_4^+SbF_6^-$ showing the highly symmetric arrangement along the z-axis with the iodine atoms in purple and the fluorine atoms in green. The "CD-Changer" pattern is due to the van-der-Waals radii of the antimony atoms that are hidden by the axial fluorine atoms. The alternation of the direction of the "Viking Hero's Skofnung Battle Axe" pattern is due to an alternation of the orientation of the IF_4 groups within the sheets.

Figure 6. A comparison of the fluorine bridging in $IF_4^+SbF_6^-$ (green) and $IF_4^+Sb_2F_{11}^-$ (yellow), showing the preferential compression of the axial F2-I1-F2A angle in the former and of the equatorial F3A-1-F2B angle in the latter.

Figure 7. A comparison of the calculated and the re-determined experimental geometries for ClF_4^+, BrF_4^+, and IF_4^+, showing the good agreement between the calculated (green) and experimental (red) data. For IF_4^+, the red values are those reported for $IF_4^+Sb_2F_{11}^-$, while the blue ones are those for $IF_4^+SbF_6^-$. The only significant deviations are caused by a preferential compression of one bond angle in each compound due to inter-ionic fluorine bridging.

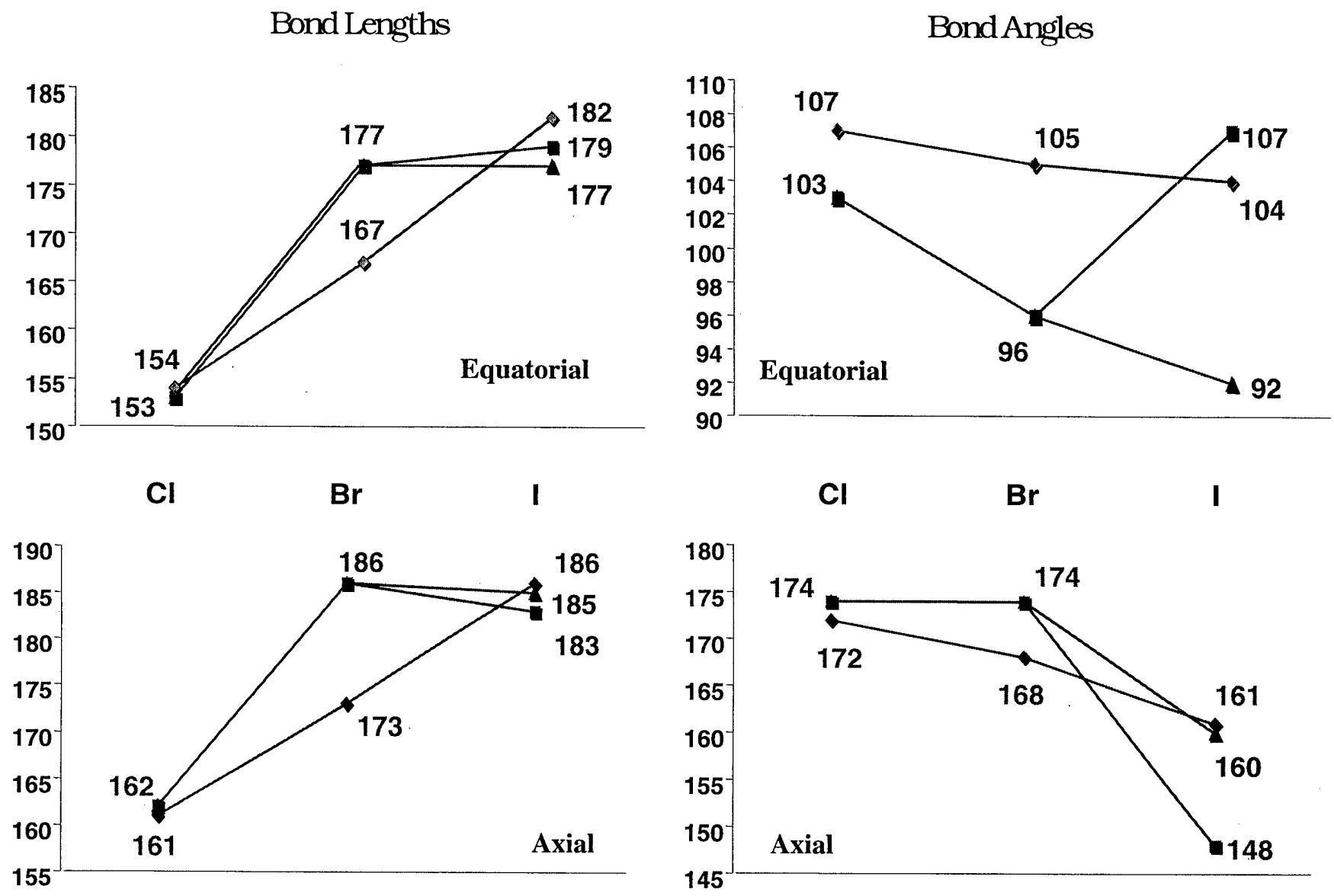
Bond Lengths
185
180
175
170
165
160
155
150
177
182
179
177
167
154
153
Equatorial
Cl
Br
I
190
185
180
175
170
165
160
155
186
186
185
183
173
162
161
Axial
Bond Angles
110
108
106
104
102
100
98
96
94
92
90
107
105
107
103
104
96
92
Equatorial
Cl
Br
I
180
175
170
165
160
155
150
145
174
174
172
168
161
160
148
Axial

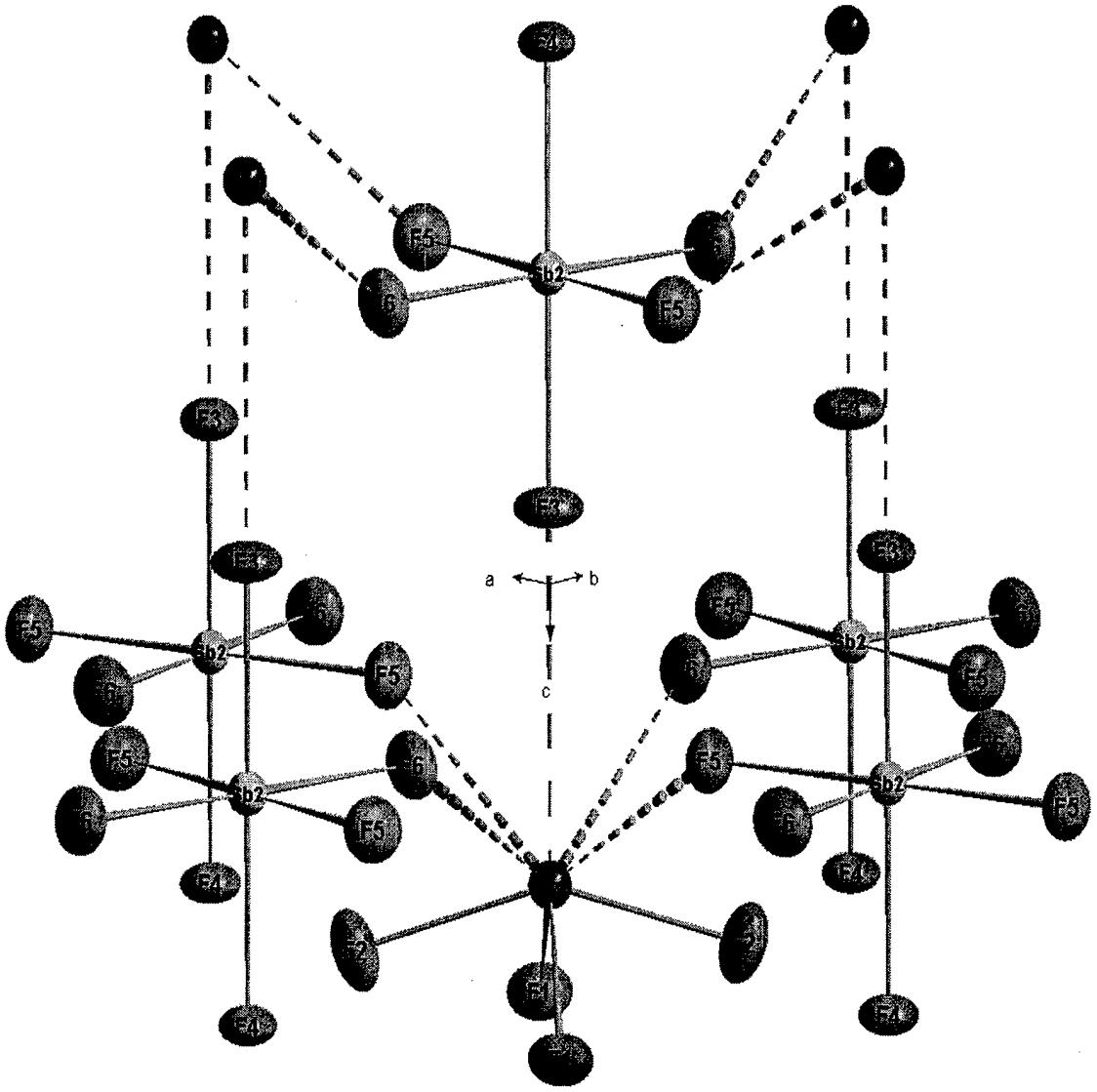
F4
F5
Sb2
F5
F3
F4
F5
a
b
c
F5
Sb2
F5
F5
Sb2
F5
F4
F2
F1
F4

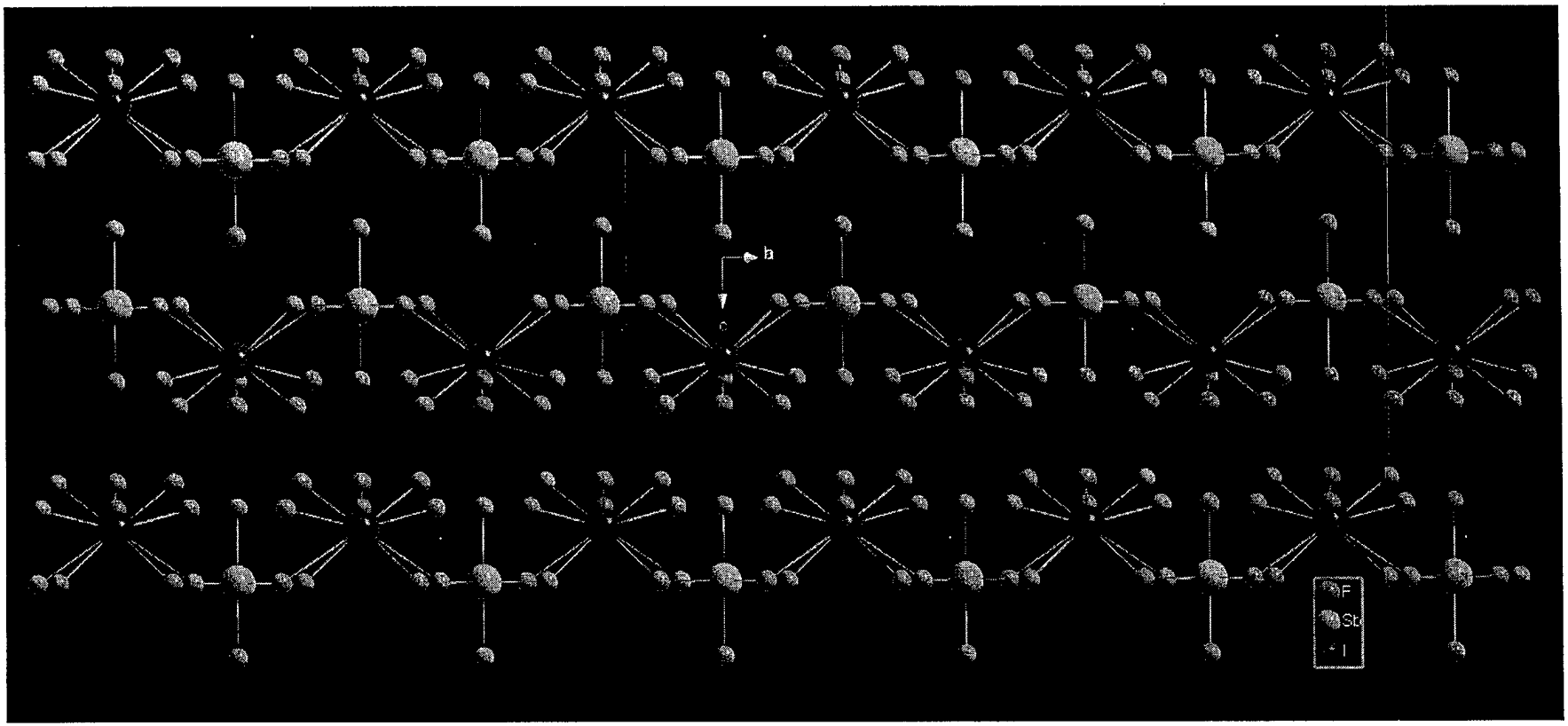
b
F
Sb

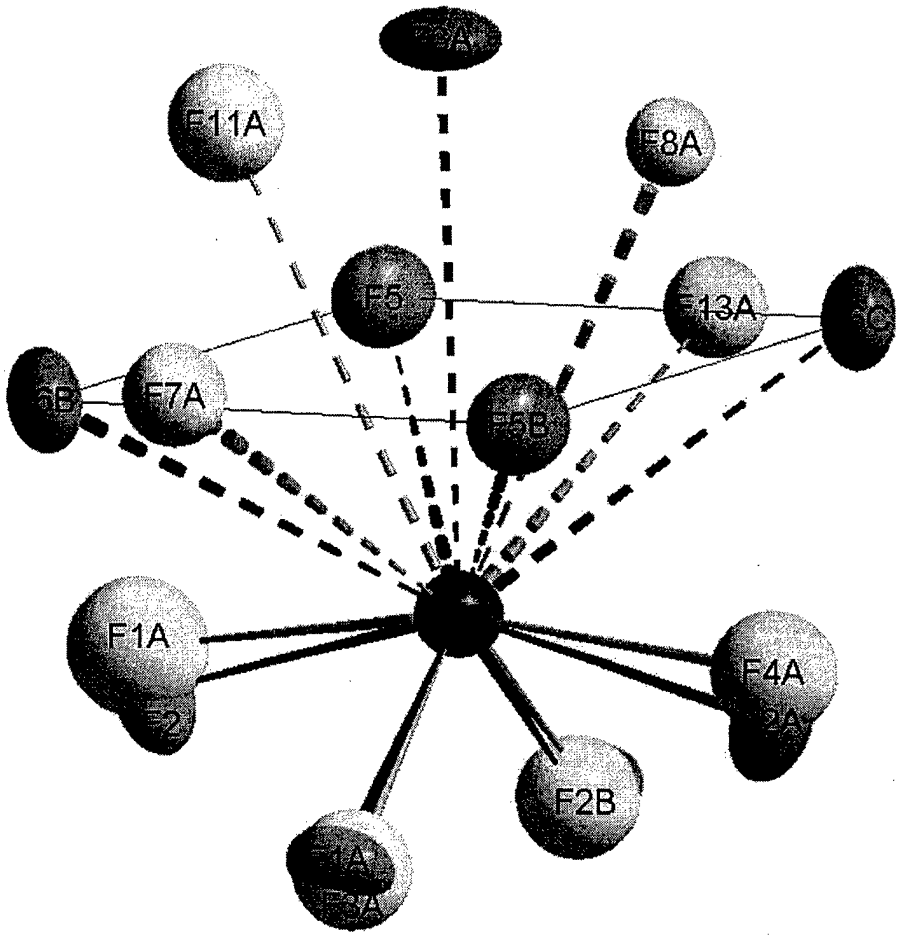
F11A
F8A
F5
F13A
F7A
F1A
F4A
F2B

Bond Lengths

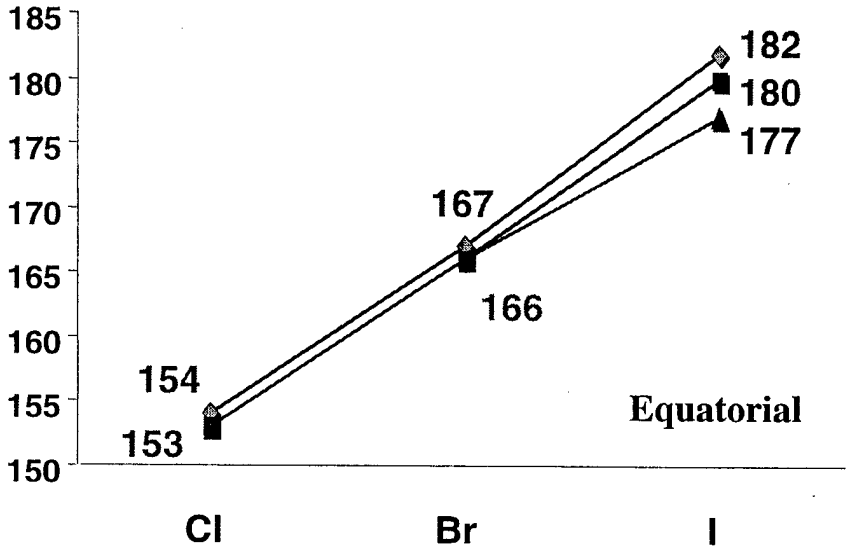

Bond Angles

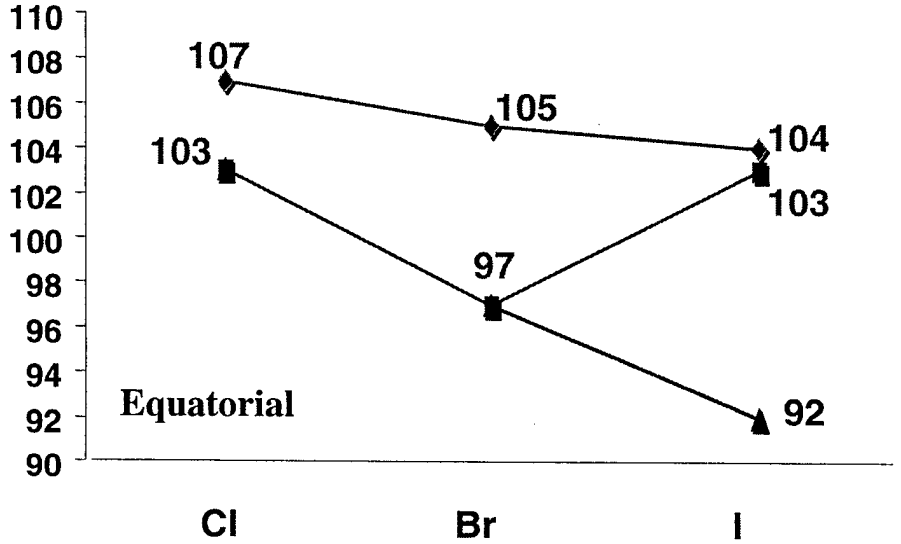

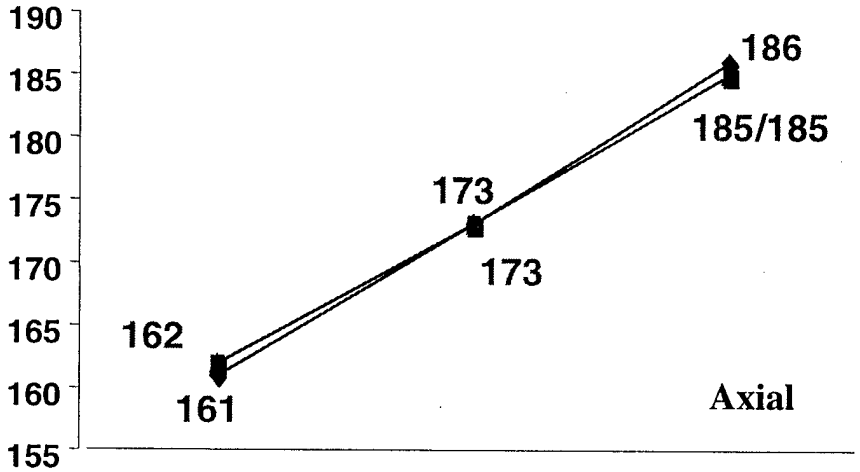

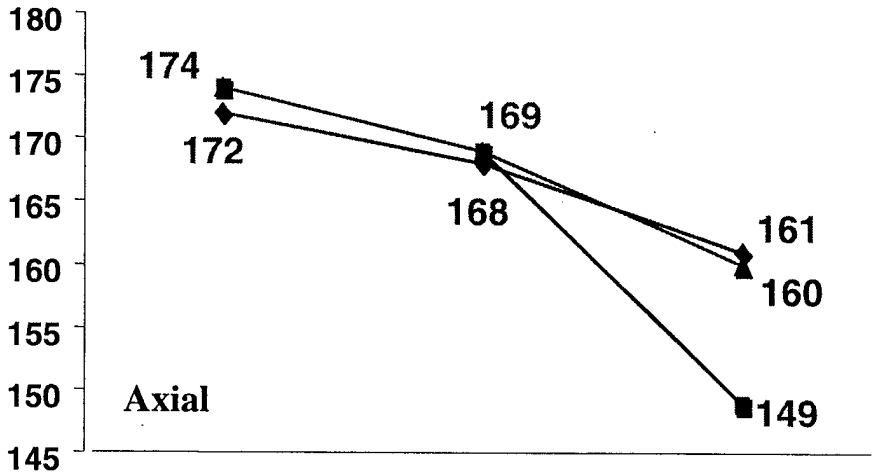

Supplementary Material

Table 1. Crystal data and structure refinement for $BrF4^{+}Sb2F11^{-}$

Identification code	BrF4Sb2F11	
Empirical formula	Br F15 Sb2	
Formula weight	608.41	
Temperature	243(2) K	
Wavelength	0.71073 Å	
Crystal system	Monoclinic	
Space group	P2(1)/c	
Unit cell dimensions	a = 5.2289(6) Å	α= 90°.
	b = 14.5095(17) Å	β= 90.280(2)°.
	c = 14.1938(17) Å	γ= 90°.
Volume	1076.9(2) $Å^3$	
Z	4	
Density (calculated)	3.753 Mg/m^3	
Absorption coefficient	8.920 mm^{-1}	
F(000)	1088	
Crystal size	0.21 x 0.18 x 0.10 mm^3	
Theta range for data collection	2.81 to 26.37°.	
Index ranges	-6<=h<=6, -13<=k<=18, -17<=l<=17	
Reflections collected	6725	
Independent reflections	2200 [R(int) = 0.0302]	
Completeness to theta = 26.37°	99.9 %	
Absorption correction	SADABS	
Max. and min. transmission	0.4691 and 0.2560	
Refinement method	Full-matrix least-squares on F^2	
Data / restraints / parameters	2200 / 0 / 164	
Goodness-of-fit on F^2	1.047	
Final R indices [I>2sigma(I)]	R1 = 0.0275, wR2 = 0.0702	
R indices (all data)	R1 = 0.0344, wR2 = 0.0735	
Extinction coefficient	0.00044(13)	
Largest diff. peak and hole	0.908 and -1.179 $e.Å^{-3}$	

Table 2. Atomic coordinates (x 10^4) and equivalent isotropic displacement parameters ($Å^2$x 10^3) for BrF4+Sb2F11-. U(eq) is defined as one third of the trace of the orthogonalized U^{ij} tensor.

	x	y	z	U(eq)
Sb(1)	5297(1)	6472(1)	3518(1)	23(1)
Sb(2)	2557(1)	8534(1)	5130(1)	22(1)
Br(1)	9167(1)	8510(1)	1861(1)	26(1)
F(1)	6574(7)	5587(2)	2720(2)	57(1)
F(2)	6881(5)	7453(2)	2865(2)	36(1)
F(3)	8081(6)	6430(2)	4312(2)	43(1)
F(4)	3511(6)	5655(2)	4262(2)	50(1)
F(5)	2400(5)	6688(2)	2798(2)	43(1)
F(6)	3984(5)	7462(2)	4366(2)	43(1)
F(7)	1149(6)	9424(2)	5882(2)	48(1)
F(8)	5461(6)	8373(2)	5849(2)	43(1)
F(9)	4238(6)	9286(2)	4287(2)	43(1)
F(10)	-224(6)	8436(2)	4329(2)	38(1)
F(11)	1073(5)	7564(2)	5847(2)	37(1)
F(12)	12022(7)	8638(2)	2465(2)	52(1)
F(13)	6324(6)	8613(2)	1243(2)	52(1)
F(14)	7971(6)	9297(2)	2590(2)	43(1)
F(15)	10410(5)	9237(2)	1077(2)	40(1)

Table 3. Bond lengths [Å] and angles [°] for BrF4+Sb2F11-.

Sb(1)-F(3)	1.837(3)	Sb(2)-F(9)	1.845(3)
Sb(1)-F(1)	1.840(3)	Sb(2)-F(10)	1.847(3)
Sb(1)-F(4)	1.844(3)	Sb(2)-F(11)	1.905(3)
Sb(1)-F(5)	1.850(3)	Sb(2)-F(6)	2.039(2)
Sb(1)-F(2)	1.892(3)	Br(1)-F(14)	1.664(3)
Sb(1)-F(6)	1.998(2)	Br(1)-F(15)	1.667(3)
Sb(2)-F(7)	1.832(3)	Br(1)-F(12)	1.728(3)
Sb(2)-F(8)	1.840(3)	Br(1)-F(13)	1.729(3)
F(3)-Sb(1)-F(1)	93.75(15)	F(8)-Sb(2)-F(10)	167.58(15)
F(3)-Sb(1)-F(4)	91.68(14)	F(9)-Sb(2)-F(10)	91.31(13)
F(1)-Sb(1)-F(4)	95.18(16)	F(7)-Sb(2)-F(11)	92.49(14)
F(3)-Sb(1)-F(5)	171.32(14)	F(8)-Sb(2)-F(11)	86.98(13)
F(1)-Sb(1)-F(5)	94.39(15)	F(9)-Sb(2)-F(11)	168.57(13)
F(4)-Sb(1)-F(5)	90.57(13)	F(10)-Sb(2)-F(11)	87.17(12)
F(3)-Sb(1)-F(2)	88.75(12)	F(7)-Sb(2)-F(6)	175.13(13)
F(1)-Sb(1)-F(2)	93.53(15)	F(8)-Sb(2)-F(6)	83.96(12)
F(4)-Sb(1)-F(2)	171.23(14)	F(9)-Sb(2)-F(6)	85.94(13)
F(5)-Sb(1)-F(2)	87.76(12)	F(10)-Sb(2)-F(6)	84.43(12)
F(3)-Sb(1)-F(6)	85.89(12)	F(11)-Sb(2)-F(6)	82.64(11)
F(1)-Sb(1)-F(6)	178.17(15)	F(14)-Br(1)-F(15)	97.48(16)
F(4)-Sb(1)-F(6)	86.63(13)	F(14)-Br(1)-F(12)	86.80(16)
F(5)-Sb(1)-F(6)	85.88(12)	F(15)-Br(1)-F(12)	85.68(15)
F(2)-Sb(1)-F(6)	84.67(11)	F(14)-Br(1)-F(13)	86.09(15)
F(7)-Sb(2)-F(8)	95.69(15)	F(15)-Br(1)-F(13)	86.78(15)
F(7)-Sb(2)-F(9)	98.94(15)	F(12)-Br(1)-F(13)	168.88(16)
F(8)-Sb(2)-F(9)	92.27(13)	Sb(1)-F(6)-Sb(2)	175.11(15)
F(7)-Sb(2)-F(10)	95.50(14)		

Symmetry transformations used to generate equivalent atoms:

Table 4. Anisotropic displacement parameters ($Å^2 x\ 10^3$) for BrF4+Sb2F11-. The anisotropic displacement factor exponent takes the form: $-2\pi^2[\ h^2\ a^{*2}U^{11} + ...\ + 2\ h\ k\ a^*\ b^*\ U^{12}\ ]$

	U^{11}	U^{22}	U^{33}	U^{23}	U^{13}	U^{12}
Sb(1)	27(1)	20(1)	21(1)	0(1)	-1(1)	0(1)
Sb(2)	26(1)	21(1)	18(1)	-1(1)	0(1)	-2(1)
Br(1)	33(1)	22(1)	22(1)	0(1)	5(1)	1(1)
F(1)	78(2)	38(2)	55(2)	-18(2)	7(2)	17(2)
F(2)	40(1)	39(2)	28(1)	9(1)	4(1)	-8(1)
F(3)	36(2)	54(2)	40(2)	8(1)	-11(1)	4(1)
F(4)	53(2)	39(2)	58(2)	17(2)	6(2)	-12(2)
F(5)	34(2)	61(2)	35(2)	2(2)	-13(1)	-5(1)
F(6)	54(2)	41(2)	36(2)	-11(1)	9(1)	13(2)
F(7)	58(2)	37(2)	49(2)	-16(2)	12(2)	6(2)
F(8)	37(2)	59(2)	32(2)	0(1)	-10(1)	-2(1)
F(9)	52(2)	41(2)	37(2)	9(1)	4(1)	-19(1)
F(10)	37(2)	43(2)	33(2)	5(1)	-10(1)	-3(1)
F(11)	46(2)	36(2)	29(1)	7(1)	5(1)	-9(1)
F(12)	55(2)	56(2)	44(2)	6(2)	-5(2)	5(2)
F(13)	48(2)	66(2)	41(2)	-2(2)	-3(2)	-4(2)
F(14)	62(2)	38(2)	30(2)	-10(1)	4(1)	17(2)
F(15)	54(2)	32(2)	33(2)	10(1)	4(1)	-6(1)

Table 5. Torsion angles [°] for BrF4+Sb2F11-.

F(3)-Sb(1)-F(6)-Sb(2)	136.6(18)
F(1)-Sb(1)-F(6)-Sb(2)	58(5)
F(4)-Sb(1)-F(6)-Sb(2)	-131.5(18)
F(5)-Sb(1)-F(6)-Sb(2)	-40.7(18)
F(2)-Sb(1)-F(6)-Sb(2)	47.4(18)
F(7)-Sb(2)-F(6)-Sb(1)	136.6(18)
F(8)-Sb(2)-F(6)-Sb(1)	-137.2(18)
F(9)-Sb(2)-F(6)-Sb(1)	-44.5(18)
F(10)-Sb(2)-F(6)-Sb(1)	47.2(18)
F(11)-Sb(2)-F(6)-Sb(1)	135.0(18)

Symmetry transformations used to generate equivalent atoms:

Table 6. Crystal Data and Structure Refinement for $IF_4^+SbF_6^-$

Identification code	IF4SBF6	
Empirical formula	F10 I Sb	
Formula weight	438.65	
Temperature	233(2) K	
Wavelength	0.71073 Å	
Crystal system	Orthorhombic	
Space group	Ibca	
Unit cell dimensions	a = 8.2702(9) Å	α= 90°.
	b = 8.3115(9) Å	β= 90°.
	c = 20.607(2) Å	γ= 90°.
Volume	1416.5(3) $Å^3$	
Z	8	
Density (calculated)	4.114 Mg/m^3	
Absorption coefficient	8.396 mm^{-1}	
F(000)	1552	
Crystal size	0.36 x 0.29 x 0.06 mm^3	
Theta range for data collection	1.98 to 26.33°.	
Index ranges	-8<=h<=10, -10<=k<=9, -25<=l<=25	
Reflections collected	3584	
Independent reflections	726 [R(int) = 0.0328]	
Completeness to theta = 26.33°	99.3 %	
Absorption correction	SADABS	
Max. and min. transmission	0.6328 and 0.1520	
Refinement method	Full-matrix least-squares on F^2	
Data / restraints / parameters	726 / 0 / 58	
Goodness-of-fit on F^2	1.187	
Final R indices [I>2sigma(I)]	R1 = 0.0241, wR2 = 0.0654	
R indices (all data)	R1 = 0.0266, wR2 = 0.0679	
Extinction coefficient	0.00289(16)	
Largest diff. peak and hole	0.897 and -0.915 $e.Å^{-3}$	

Table 7. Atomic Coordinates (x 10^4) and Equivalent Isotropic Displacement Parameters ($Å^2$x 10^3) for $IF_4^+SbF_6^-$. U(eq) is Defined as One Third of the Trace of the Orthogonalized U^{ij} Tensor.

	x	y	z	U(eq)
I(1)	5000	2500	1505(1)	16(1)
Sb(2)	0	2500	857(1)	13(1)
F(1)	3786(2)	1313(2)	2048(1)	27(1)
F(2)	3490(2)	4031(2)	1743(1)	32(1)
F(3)	0	2500	-42(2)	29(1)
F(4)	0	2500	1752(2)	25(1)
F(5)	2238(2)	2069(2)	857(1)	28(1)
F(6)	439(2)	4725(2)	853(1)	28(1)

Table 8. Bond Lengths [Å] and Angles [°] for $IF_4^+SbF_6^-$.

I(1)-F(1)#1	1.7981(17)	Sb(2)-F(3)	1.853(4)
I(1)-F(1)	1.7981(17)	Sb(2)-F(6)#2	1.8846(17)
I(1)-F(2)	1.8490(17)	Sb(2)-F(6)	1.8846(17)
I(1)-F(2)#1	1.8490(17)	Sb(2)-F(5)#2	1.8854(17)
Sb(2)-F(4)	1.845(3)	Sb(2)-F(5)	1.8854(17)

F(1)#1-I(1)-F(1)	103.06(12)	F(6)#2-Sb(2)-F(6)	179.53(12)
F(1)#1-I(1)-F(2)	80.48(9)	F(4)-Sb(2)-F(5)#2	90.00(6)
F(1)-I(1)-F(2)	80.53(8)	F(3)-Sb(2)-F(5)#2	90.00(6)
F(1)#1-I(1)-F(2)#1	80.53(8)	F(6)#2-Sb(2)-F(5)#2	89.82(7)
F(1)-I(1)-F(2)#1	80.48(9)	F(6)-Sb(2)-F(5)#2	90.18(7)
F(2)-I(1)-F(2)#1	149.24(13)	F(4)-Sb(2)-F(5)	90.00(6)
F(4)-Sb(2)-F(3)	180.0	F(3)-Sb(2)-F(5)	90.00(6)
F(4)-Sb(2)-F(6)#2	90.24(6)	F(6)#2-Sb(2)-F(5)	90.18(7)
F(3)-Sb(2)-F(6)#2	89.76(6)	F(6)-Sb(2)-F(5)	89.82(7)
F(4)-Sb(2)-F(6)	90.24(6)	F(5)#2-Sb(2)-F(5)	179.99(12)
F(3)-Sb(2)-F(6)	89.76(6)		

Symmetry transformations used to generate equivalent atoms:

#1 -x+1,-y+1/2,z+0 #2 -x+0,-y+1/2,z+0

Table 9. Anisotropic Displacement Parameters ($Å^2 x\ 10^3$) for $IF_4^+SbF_6^-$. The Anisotropic Displacement Factor Exponent Takes the Form: $-2\pi^2[\ h^2\ a^{*2}U^{11} + ...\ + 2\ h\ k\ a^*\ b^*\ U^{12}\ ]$

	U^{11}	U^{22}	U^{33}	U^{23}	U^{13}	U^{12}
I(1)	17(1)	15(1)	16(1)	0	0	-1(1)
Sb(2)	14(1)	13(1)	13(1)	0	0	0(1)
F(1)	34(1)	28(1)	21(1)	5(1)	3(1)	-9(1)
F(2)	29(1)	24(1)	45(1)	-5(1)	9(1)	5(1)
F(3)	38(2)	38(2)	11(2)	0	0	8(1)
F(4)	31(2)	32(2)	11(2)	0	0	-1(1)
F(5)	18(1)	35(1)	30(1)	1(1)	1(1)	5(1)
F(6)	36(1)	16(1)	33(1)	1(1)	2(1)	-4(1)

Structures of the BrF_4^+ and IF_4^+ Cations

Ashwani Vij, Fook S. Tham, Vandana Vij,
William W. Wilson, and Karl O. Christe*

The large discrepancies between the calculated and previously observed structures for BrF_4^+ and IF_4^+ have now been resolved. A re-determination of the crystal structures of $BrF_4^+Sb_2F_{11}^-$ and $IF_4^+SbF_6^-$ shows that the large differences were mainly due to large errors in the original experimental data. The general agreement between the calculated and the redetermined geometries of BrF_4^+ and IF_4^+ is excellent, except for the preferential compression of one bond angle in each ion due to the influence of inter-ionic fluorine bridges. In BrF_4^+, the fluorine bridges compress the equatorial angle. In IF_4^+, the nature of the fluorine bridges depends on the counter ion and either the axial or the equatorial bond angle is preferentially compressed.